THE JOURNAL OF PHYSICAL CHEMISTRY A

Article

pubs.acs.org/JPCA

Photoelectron Spectroscopy and Ionic Fragmentation of $OSeCl_2$ and Its Analogue $OSCl_2$ under VUV Irradiation

Mariana Geronés,[†] Lucas S. Rodríguez Pirani,[†] Mauricio F. Erben,[†] Rosana M. Romano,[†] Reinaldo L. Cavasso Filho,[‡] Sheng Rui Tong,[§] Maofa Ge,[§] and Carlos O. Della Védova*[,†]

[†]CEQUINOR (CONICET-UNLP), Departamento de Química, Facultad de Ciencias Exactas, Universidad Nacional de La Plata, C. C. 962 (1900) La Plata, República Argentina

[‡]Universidade Federal do ABC, Rua Catequese, 242, CEP 09090-400 Santo André, São Paulo, Brazil

[§]State Key Laboratory for Structural Chemistry of Unstable and Stable Species, Beijing National Laboratory for Molecular Sciences (BNLMS), Institute of Chemistry, Chinese Academy of Sciences, Beijing 100080, People's Republic of China

Supporting Information

ABSTRACT: The electronic structure and the dissociative ionization of selenium oxychloride, $OSeCl_2$, have been investigated in the valence region by using results from both photoelectron spectroscopy (PES) and synchrotron-based photoelectron photoion coincidence (PEPICO) spectra. The PES is assigned with the help of quantum chemical calculations at the outer-valence Green's function (OVGF) and symmetry adapted cluster/configuration interaction (SAC-CI) levels. The first energy ionization is observed at 11.47 eV assigned to the ionization of electrons formally delocalized over the Se, Cl, and O lone pair orbitals. Irradiation of $OSeCl_2$ with photons in the valence region leads to the formation of $OSeCl_2^{\bullet+}$, $OSeCl^+$, $SeCl_2^{\bullet+}$, $SeCl^+$, and $SeO^{\bullet+}$ ions. Furthermore, the inner shell Se 3p, Cl 2p, and Se 3s electronic regions of $OSeCl_2$ together with S 2p, Cl 2p, and S 2s electronic regions of thionyl chloride, $OSCl_2$, have been studied by using tunable synchrotron radiation. Thus, total ion yield spectra and the fragmentation patterns deduced from PEPICO spectra at the various excitation energies have been studied. Cl^+, $O^{\bullet+}$, and $Se^{\bullet+}$ ions appear as the most intense fragments in the $OSeCl_2$ PEPICO spectra, like in the sulfur analogue $OSCl_2$, whose photofragmentation is dominated by the Cl^+, $O^{\bullet+}$, and $S^{\bullet+}$ ions. Fragmentation processes in $OSCl_2$ leading to the formation of the double coincidences involving atomic ions appear as the most intense in the PEPIPICO spectra.

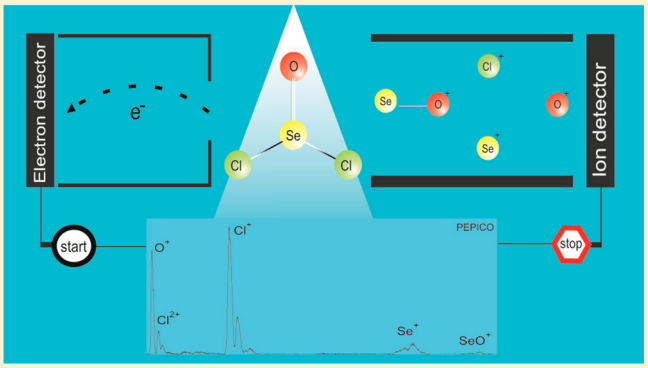

1. INTRODUCTION

Experimental gas-phase studies on fundamental aspects of selenium-containing compounds, including spectroscopic and kinetic properties, are scarce. This is not surprising because this kind of substance is usually an unstable species, and is difficult to obtain in pure form. Moreover, generally they are toxic compounds with unpleasant odors.[1]

The photoionization behavior of clusters of selenium were thoroughly investigated by Hayakawa et al.[2,3] Multiply charged Se^{z+} ions are produced after Se K-shell excitation (12.6 keV X-ray photons), as determined by PEPICO analysis. It is postulated that the atomic ions are produced by Coulomb explosion processes, with the branching ratios being dependent on the size of the clusters.[4,5]

Further reports on the electronic structure of selenium-containing species are available in the literature, including the photoelectron spectra of the simple triatomic H_2Se,[6] OCSe, SCSe, and SeCSe molecules in the gas-phase.[7−9] Comparisons between the selenium and sulfur analogues are usually performed to gain information on the specific characteristics of the electronic structure related to the chalcogen atom involved in the chemical bond. The fragmentation pathways of ionized diselenides (RSe−SeR) and selenosulfenates (RSe−SR, R = alkyl group) under electron impact were analyzed by time-of-flight mass spectrometry, showing the preference for the rupture of the Se−C bond, together with the Se−Se and Se−S bonds for diselenides and selenosulfenates, respectively.[10] Very recently, the unimolecular dissociation of energy selected dimethyldisulfide and dimethyl diselenide was studied using imaging photoelectron photoion coincidence (iPEPICO) spectroscopy.[11] XH-, CH_3-, and CH_nX-loss reactions (n = 2−4, X = S, Se) were observed in both molecules with varying branching ratios. The SH-loss from dimethyldisulfide and the SeH-loss from dimethyldiselenide are found to be slow dissociations which proceed through a tight transition state. In both samples, the CH_3-loss is a fast dissociative photo-

Received: March 5, 2015
Revised: June 30, 2015
Published: July 2, 2015

DOI: 10.1021/acs.jpca.5b02162
J. Phys. Chem. A 2015, 119, 8000−8009

ionization process at threshold. At low energies, the formation of CH_2S^+ and CH_4S^+ from CH_3S-SCH_3 occurs through a common, fairly loose transition state. At higher energies, the symmetric breaking of the molecule into two CH_3S^+ fragments also occurs via two H-transfer transition states. In $CH_3Se-SeCH_3$, a similar mechanism can be seen, although the relative abundance of these corresponding ions does not rise as rapidly since these channels are outcompeted by the methyl-loss channel. Recently, the inner-shell photoionization of CH_3SeH and CH_3CH_2SeH was studied by using an intense (>10^{17} W/cm^2) X-ray free-electron laser as source of 5 fs X-ray pulses with photon energies in the keV range in conjunction with detection techniques based on coincidence ion momentum spectroscopy. Signatures of charge redistribution across the molecules were observed, especially for the larger ethylselenol molecule. Moreover, from the kinetic energy distribution of the ionic fragments, details of the Coulomb explosion processes were revealed.[12,13] Studies concerning shallow- and inner-core electrons in sulfur-containing compounds as well as studies in the valence region have been analyzed by our research group by using synchrotron radiation and multicoincidence techniques.[14,15]

Following these analyses, we became interested in molecules constituted by formal chalcogen substitution, i.e., the selenium analogues of the sulfur species. To our knowledge, synchrotron-based studies on the Se 3p and/or 3s shallow-core level for gas-phase selenium-containing molecules have not been performed up to now. Thus, a simple and stable species, selenium oxychloride, was the first molecule chosen to be studied. In the present work, the electronic structure of selenium oxychloride, $OSeCl_2$, in both the valence and inner-shell regions was investigated using synchrotron-based experimental techniques and HeI photoelectron spectroscopy (PES). The total ion yield spectrum (TIY) and the photoelectron−photoion coincidence (PEPICO) spectra at selected photon energies, using synchrotron radiation in the valence region and in the inner-shell Se 3p, Cl 2p, and Se 3s electron region, have been measured.

The molecular geometry of selenium oxychloride has been studied by electron diffraction.[16,17] A previous study of the Raman spectrum agrees with the fact that $OSeCl_2$ has a pyramidal structure in the liquid-phase. The matrix isolation study concerning the investigation of the IR bands of $OSeCl_2$ above 90 cm^{-1} has been reported.[16] In contrast with an earlier IR work on $OSeCl_2$, all six of the allowed IR bands by the point group C_s were found.[18] Due to some particular properties, including a high dielectric constant, high specific conductance, and its dissolving ability, $OSeCl_2$ is an excellent compound as a solvent for many kind of reactions.[19]

To compare with the $OSeCl_2$, we extend in the present work the synchrotron photoionization investigations to the sulfur analogue, $OSCl_2$. Thionyl chloride is a powerful chlorinating reagent primarily used in the industrial production of organochlorine compounds, which are often intermediates in pharmaceuticals and agrochemicals.[20−22] A porous carbon current collector filled with thionyl chloride is used as a liquid cathode in the high-tech lithium-thionyl chloride batteries (Li/$OSCl_2$).

In its fundamental electronic state, $OSCl_2$ also adopts a pyramidal molecular geometry with C_s molecular symmetry. From a spectroscopic point of view, photoabsorption spectra of $OSCl_2$ as well as partial-ion-yield measurements have been reported for both the S and Cl K-edges.[23,24] However, to our knowledge, the electronic properties corresponding to the sulfur and chlorine 2p-edges and ionic fragmentation of $OSCl_2$ in these energy regions have not been previously described and therefore constitute also a scope of the present work.

2. EXPERIMENTAL SECTION

2.1. Photoionization by Using Tunable Synchrotron Radiation. The experiments were performed in two campaigns using the TGM (toroidal grating monochromator) beamline at the Laboratório Nacional de Luz Síncrotron (LNLS), Campinas São Paulo, Brazil.[25,26] This monochromator operates in the range 12−300 eV and provides linearly polarized light monochromatized with resolution power better than 400 and with a photon energy resolution from 12 to 21.5 eV of $E/\Delta E$ = 550.[27−29] The intensity of the emergent beam is recorded by a light-sensitive diode. High-purity vacuum-ultraviolet photons are used provided by the gas-phase harmonic filter to avoid contamination of the photon beam with high-order harmonics.[28,29]

The beam intersects the effusive gaseous sample inside a high vacuum chamber, with base pressure in the range 10^{-8} mbar. The working pressure was maintained below 2× 10^{-6} mbar during data acquisition. The ions produced by the interaction of the gaseous sample with the light beam were detected using a time-of-flight (TOF) mass spectrometer of the Wiley−MacLaren type.[30−32] The axis of the TOF spectrometer was perpendicular to the photon beam and parallel to the plane of the storage ring. Electrons were attracted toward the multichannel plate (MCP) and detected without energy analysis. This event starts the flight time determination process of the corresponding ion, which is consequently accelerated in opposite direction and detected by the ion MCP which provides the stop signals to the time-to-digital converter (TDC). The ions produced up to three stop signals for a time-to-digital converter (TDC) started by the signal from one of the electrons accelerated in the opposite direction. The mass spectra containing mainly contributions from single ionization processes were obtained using the correlation between one electron and an ion generated at the same ionization event (photoelectron−photoion coincidence (PEPICO) technique). In addition, the photoelectron photoion photoion coincidence (PEPIPICO) spectra can be obtained simultaneously. These last spectra have ions from multiple ionizations where the two lightest ions which arrive coincidentally with photoelectrons would be detected.

The samples of selenium oxychloride and thionyl chloride were obtained commercially as 97% pure liquids from Sigma-Aldrich. The liquid samples were purified by repeated trap-to-trap vacuum distillation. The final purity of the compounds in both vapor- and liquid-phases was checked by IR spectroscopy.[18] The purified compounds were stored and transported in vacuum flame-sealed tubes, and special care was taken to avoid hydrolysis and oxidation reactions by minimizing the contact with air.

2.2. Photoelectron and Photoionization Mass Spectroscopies (PES and PIMS). The UV PE spectrum of $OSeCl_2$ was obtained in the double chamber UPS-II apparatus equipped with a helium discharge lamp which emits a wavelength of 58.4 nm (corresponding to an energy of 21.2 eV), and the operational resolution obtained from the $Ar^{\bullet+}$ ($^2P_{3/2}$) peak was ∼35 meV. Calibration of the spectra was achieved by admitting the sample studied into the spectrometer at the same time as argon and methyl iodide.[33−39] Mass analysis

DOI: 10.1021/acs.jpca.5b02162
J. Phys. Chem. A 2015, 119, 8000−8009

of ions was performed with the time-of-flight mass analyzer mounted directly to the photoionization sector.[40] The ionization was provided by single-wavelength HeI radiation. The PE and PIM spectra were recorded within seconds of each other under identical conditions.

Vertical ionization energies (IEs) were calculated using the symmetry adapted cluster/configuration interaction (SAC-CI) method[41,42] and the outer-valence Green's function (OVGF) calculations.[43] All calculations were performed with the Gaussian 03 quantum chemistry package and the 6-311+G(d) basis set.[44]

3. RESULTS AND DISCUSSION

3.1. Photoelectron Spectra. The HeI PE spectrum of $OSeCl_2$ is given in Figure 1, and in Table 1 the experimental

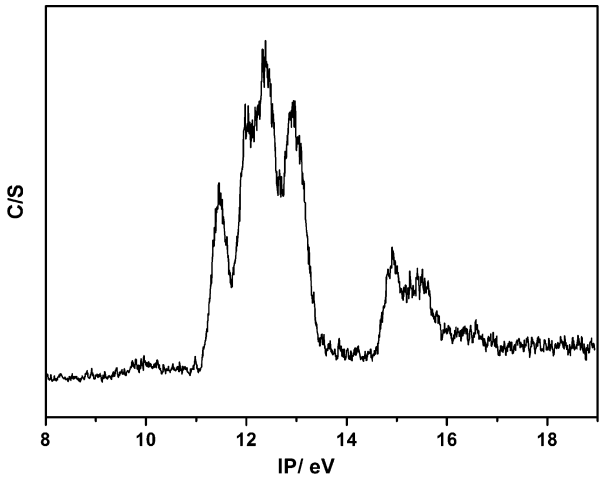

Figure 1. HeI photoelectron spectrum of $OSeCl_2$.

and theoretical [OVGF/6-311+G(d) and SAC-CI/6-311+G(d)] vertical ionization energies (IEs) are included. The main characters of the 11 highest occupied molecular orbitals of $OSeCl_2$ are also shown (Figure S1 in the Supporting Information). The HeI PES of the related compound $OSCl_2$ was previously recorded by Chadwic et al.,[45] and the experimental ionization energies are also listed in Table 1 together with the ionization energies calculated in this work. In addition, in Table 1 the OVGF pole strengths are presented and can be seen that all are larger than 0.85, which is consistent with a one-electron depiction of ionization.[46−49]

The molecule $OSeCl_2$ belongs to the C_s symmetry group which has only two molecular orbital irreducible representations, a′ (σ in-plane orbitals) and a″ (π out-of-plane orbitals). Their 26 valence electrons are arranged in 13 doubly occupied orbitals, and in an independent particle description its electronic configuration is

$$OSeCl_2,\ (core)^{50}(a')^2(a'')^2(a'')^2(a')^2(a')^2(a'')^2(a')^2(a'')^2\text{-}(a')^2(a')^2(a'')^2(a')^2(a')^2$$

In the HeI PE spectrum, well-defined bands associated with ionization processes from occupied molecular orbitals can be observed. From Table 1, it can be seen that an excellent consistency between the experimental energies and OVGF calculated ionization energies exists for both molecules. The agreement between theory, using the SAC-CI method, and experiment is excellent in the case of $OSCl_2$, but deviations

Table 1. Experimental and Calculated Ionization Energies and MO Characters for $OSeCl_2$ and $OSCl_2$

$OSeCl_2$					
PES (eV)	SAC-CI (eV)[a]	OVGF (eV)[b,c]	symmetry	MO	character
11.47 ± 0.01	10.98	11.57 (0.92)	a′	(38)	n(Se), n(O), n(Cl)
11.9 ± 0.4	11.73	12.05 (0.91)	a″	(37)	n(Cl), n(O)
12.17	11.93	12.20 (0.92)	a″	(36)	n(Cl), n(O)
12.4 ± 0.4	12.09	12.44 (0.91)	a′	(35)	n(Cl), n(O)
12.93 ± 0.01	12.56	12.89 (0.90)	a″	(34)	n(Cl), n(O)
	12.71	12.91 (0.91)	a′	(33)	n(Cl), n(O)
15.0 ± 0.4	14.95	16.07 (0.92)	a′	(32)	σ (OSe)
$OSCl_2$					
PES (eV)[d]	SAC-CI (eV)[a]	OVGF (eV)[b,c]	symmetry	MO	character
11.30	11.12	11.43 (0.91)	a′	(29)	n(S), n(O), n(Cl)
11.90	11.89	11.76 (0.90)	a″	(28)	n(Cl), n(O)
12.21	12.10	12.25 (0.90)	a″	(27)	n(Cl), n(O)
12.55	12.39	12.49 (0.90)	a′	(26)	n(Cl), n(O)
13.04	12.83	12.97 (0.89)	a″	(25)	n(Cl), n(O)
	12.95	13.18 (0.90)	a′	(24)	n(Cl), n(O)
16.00	16.12	17.19 (0.91)	a′	(23)	σ (OS)

[a]Calculated values at the SAC-CI/6-311+G(d) level of approximation with B3LYP/6-311+G(d) optimized geometry. [b]Calculated values at the OVGF/6-311+G(d) level of approximation with B3LYP/6-311+G(d) optimized geometry. [c]Pole strength in parentheses. [d]Values from ref 46.

from the experimental values between 0.49 and 0.1 eV can be observed for ionization energies below 15.0 eV corresponding to the $OSeCl_2$ molecule. It is plausible that the use of more complete basis sets is required for better performance of SAC-CI calculations on selenium compounds.

For $OSeCl_2$, the first vertical ionization energy at 11.47 eV was assigned to the ionization process mainly from the selenium lone pair orbital (n(Se)). A series of three overlapped bands are observed in the 11.8−13 eV region. A signal located at around 11.9 eV and the following two bands found at 12.2 and 12.4 eV could be related to the electron ionization of mainly chlorine lone pair orbitals (n(Cl)) (corresponding to the MO 37, MO 36, and MO 35 in Table 1 and Supporting Information Figure S1). According to the theoretical calculation, the band observed at 12.93 eV is associated with the ionization processes caused by an electron ejected from an n(O) orbital and of an electron ejected from the remaining chlorine lone pair orbital. In the high ionization energy region (>13.00 eV), the 15.01 eV feature in the PES is related to an ionization process of bonded electrons from the σ_{Se-O} orbital.

According to the calculations [UB3LYP/6-311+G(d)] performed to analyze the nature of the low-lying cationic radical formed in the first ionization process, the initial charge distribution (Mulliken atomic charges) for the free molecule is affected upon ionization from 0.511 to 0.527 at the Se atom, from −0.393 to −0.067 at the O atom, and from −0.059 to 0.270 in each of the Cl atoms.

The HeI PES of the related compound $OSCl_2$,[46] below 17 eV, consists of six well-defined bands located at 11.30, 11.90,

DOI: 10.1021/acs.jpca.5b02162
J. Phys. Chem. A 2015, 119, 8000−8009

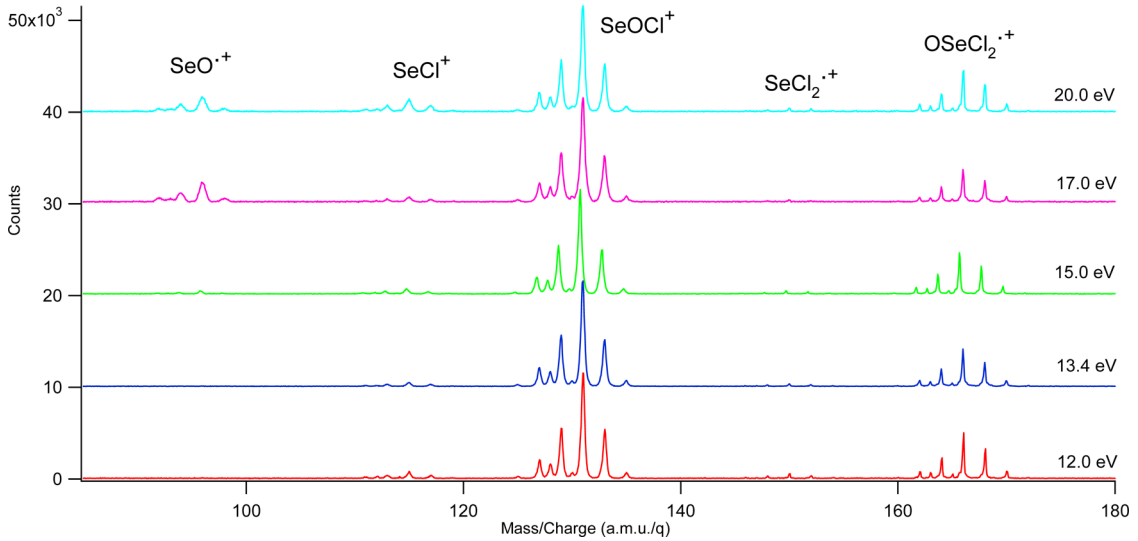

Figure 2. PEPICO spectra of $OSeCl_2$ at selected irradiation energies in the valence region.

12.21, 12.55, 13.04, and 16.00 eV. Chadwic et al.[46] assigned the spectrum of $OSCl_2$ on the basis of PES results of similar molecules; therefore, that assignment was tentative. Our assignment of the bands with the assistance of the higher-level quantum chemical calculations based on the SAC-CI and OVGF methods allows a better description of this ionization processes on the basis of one-particle description, which is general agreement with the reported assignment for thionyl chloride.

The ultraviolet photoionization mass spectrum (PIMS) of $OSeCl_2$ is shown in Figure S2 (see in the Supporting Information). The photofragmentation of $OSeCl_2$ ionized by using HeI radiation is dominated by a rupture process involving the Se−Cl single bond. Thus, the $OSeCl^+$ ion represents the most important photoproduct after 21.2 eV irradiation. The next most abundant ions are $OSeCl_2^{\bullet+}$ and $SeCl_2^{\bullet+}$. Finally, weak signals for the $SeO^{\bullet+}$ and $SeCl^+$ fragments also appear in this spectrum indicating low relative abundance. The characteristic selenium and chlorine natural isotopomeric distribution can be seen in the PIMS spectrum.

3.2. Photoionization in the Valence Region. A series of PEPICO spectra taken at fixed photon energies in the range 11−20 eV for $OSeCl_2$, together with a fragment assignment of the bands are shown in Figure 2. Naturally occurring isotopomer fragments, mainly due to the presence of ^{74}Se, ^{76}Se, ^{77}Se, ^{78}Se, ^{80}Se, ^{82}Se, ^{35}Cl, and ^{37}Cl isotopes, are noticeably observed due to the suitable mass resolution attained in the experiments. This fact assists the assignment of the ion fragments appearing in the coincidence spectra. The branching ratios for ion production obtained from the PEPICO spectra are given in Table 2. The quantum chemically estimated double ionization threshold at the UB3LYP/6-311+G* level of approximation for $OSeCl_2$ is computed at 28.41 eV of energy. Therefore, no contribution of double ionization processes is expected in the range of energy used.

The parent ion as well as fragment ions were detected. When the sample is irradiated with photons of 12.0 eV, the $OSeCl^+$ signal dominates the spectra (71% approximately) followed in abundance by the signal originated by the molecular ion (19% approximately). The $SeCl_2^{\bullet+}$ and $SeCl^+$ species are also discernible in this spectrum. The first ionization energy of the $OSeCl_2$ molecule (11.47 eV, see Table 1) is lower than 12.0 eV (the lowest energy delivered by the TGM beamline), being possible to observe in this spectrum ionization processes from MO 38 and MO 37 corresponding to lone pair electrons nominally located on the selenium, oxygen, and chlorine atoms.

Table 2. Branching Ratios (%) for Fragment Ions Extracted from PEPICO Spectra Taken at Photon Energies in the Valence Region for $OSeCl_2$ and $OSCl_2$[a]

	$OSeCl_2$				
	photon energy (eV)				
branching ratios for selected ions	12.0	13.4	15.0	17.0	20.0
$SeO^{\bullet+}$			8.2	17.4	17.5
$SeCl^+$	7.3	7.2	9.6	7.6	10.5
$OSeCl^+$	71.2	72.7	62.7	57.9	56.2
$SeCl_2^{\bullet+}$	1.6	1.4	1.6	1.4	1.4
$OSeCl_2^{\bullet+}$	19.9	18.8	17.9	14.1	14.2
	$OSCl_2$				
	photon energy (eV)				
branching ratios for selected ions	12.0	15.0	16.0	17.0	20.0
Cl^+					5.6
SO^+			9.0	25.0	24.0
SCl^+					4.8
$OSCl^+$	81.0	75.0	67.0	52.0	40.0
$OSCl_2^{\bullet+}$	12.9	14.6	14.9	15.3	16.8

[a]Signals for the $HCl^{\bullet+}$ and $SO_2^{\bullet+}$ ions are not listed. Contributions of the natural isotopomers of Cl and Se natural are summed together. The estimated experimental error was 10%.[52,53]

A schematic representation of the energies of different pathways for the ionic dissociation of the parent ion ($OSeCl_2^{\bullet+}$) considering the rupture of only one chemical bond is given in Figure 3. Calculated dissociation channels leading to the formation of $OSeCl^+$, $SeCl_2^{\bullet+}$, and $SeCl^+$ are energetically more favored than the dissociation pathway leading to the formation of Cl^+, $O^{\bullet+}$, and OCl^+, respectively. This is in qualitative agreement with the behavior observed in the PEPICO spectra (Figure 2).

At photon energy near 15.0 eV, the ionization channel for the formation of $SeO^{\bullet+}$ is opened, and this fragment can be observed with a relative intensity of 8% approximately. Irradiation of $OSeCl_2$ with photons of 17.0 eV leads to an

DOI: 10.1021/acs.jpca.5b02162
J. Phys. Chem. A 2015, 119, 8000−8009

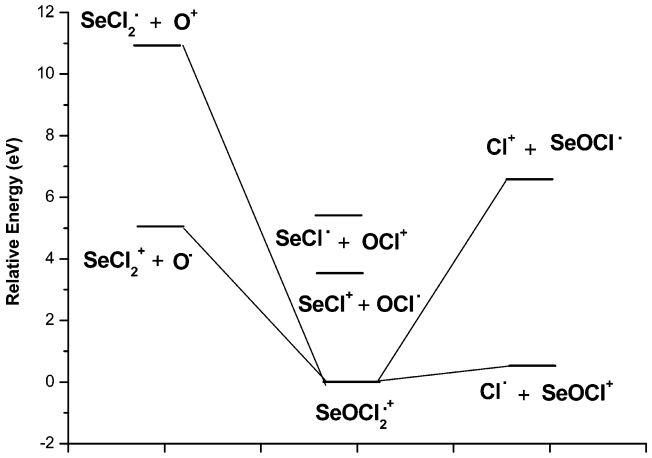

Figure 3. Energy profiles for dissociation of the molecular ion $OSeCl_2^{\bullet+}$ calculated with the UB3LYP/6-311+G(d) approximation.

increment in the intensity of this last ion. In comparison with $OSeCl_2$, the PEPICO spectra of its analogue $OSCl_2$ have also been recorded in this work, and the branching ratios for ion production obtained from the PEPICO spectra are given in Table 2. Furthermore, the threshold photoelectron photoion coincidence (TPEPICO) spectroscopy of $OSCl_2$ supersonically cooled was studied by Mayer and Baer.[50] The formation of $OSCl^+$ ion also dominates the dissociative photoionization of the low-lying cationic state, and the appearance energy of the $OSCl^+$ ion was to be 11.73 ± 0.01 eV, which leads to their $OSCl_2^{\bullet+}$ heat of formation of 802 ± 1 kJ/mol. More recently, time-of-flight spectra of energy selected $OSCl_2$ ions were collected in the photon energy range 11.0−16.0 eV with the iPEPICO instrument.[51] Modeling the first chlorine-loss dissociation of the $OSCl_2^{\bullet+}$ molecular ion results in a 0 K appearance energy of 11.709 ± 0.003 eV for the $OSCl^+$ ion.

In the PEPICO spectrum obtained at 12.0 eV (Figure 4), a major contribution of the $OSCl^+$ ion is observed (80% approximately) together with a signal corresponding to the parent molecular ion ($OSCl_2^{\bullet+}$) (12% approximately). When the photon energy reaches a value near 16.0 eV, the ionization channel for the formation of SO^+ is opened having a relative intensity of 9%. In addition, when the sample is irradiated with photons of 17.0 eV, a marked enhancement in the intensity of this signal could be observed. At 20 eV, access is gained to ionization channels for the production of the ions Cl^+ and SCl^+ from ionized states of $OSCl_2^{\bullet+}$. Signals for the $HCl^{\bullet+}$ and $SO_2^{\bullet+}$ ions, due to the decomposition of the sample, also appear in all these spectra, having a very weak relative intensity.

3.3. Photoionization in the Shallow-Core Regions.

3.3.1. Total Ion Yield Spectra (TIY) of $OSeCl_2$. The TIY spectra were obtained by recording the count rates of the total ions (parent and fragment ions) as a function of the incident photon energy. At energies corresponding to shallow and core−shell electronic levels, the TIY is a powerful method to be used as a complement to the absorption spectroscopy.[54] The TIY spectrum of $OSeCl_2$ obtained in the photon energy range 150.0−250.0 eV is depicted in Figure S3 (see in the Supporting Information). The selenium 3p and 3s regions together with the chlorine 2p-edge could be observed in this spectrum.

As can be seen below the Se 3p threshold (located at approximately 180.0 eV), the spectrum exhibits two signals at 164.0 and 169.2 eV which should correspond to transitions involving the spin−orbit splitting of the 3p term of selenium into $3p_{1/2}$ and $3p_{3/2}$ levels. In addition, a third broad signal emerges as a low-intensity band at approximately 166.0 eV. In the vicinity of the Cl 2p-edge, two broad signals located at 198.5 and 200.1 eV are observed. The observed resonance transitions may be mainly assigned to transitions involving the spin−orbit split of the 2p term in the $2p_{1/2}$ and $2p_{3/2}$ levels of the excited chlorine species toward the unoccupied σ^*_{Se-Cl} antibonding orbitals (Figure S4 in the Supporting Information). In addition, the Se 3s-edge can be observed at 235.0 eV in the TIY spectrum of Supporting Information Figure S3. In addition, we have recorded the total ion yield (TIY) spectrum of $OSeCl_2$ near the Se 3d-edge. Two broad and weak resonances are observed at 52.9 and 53.9 eV approximately and may correspond to transitions involving the spin−orbit split of the Se 3d term in the $3d_{3/2}$ and $3d_{5/2}$ levels in the

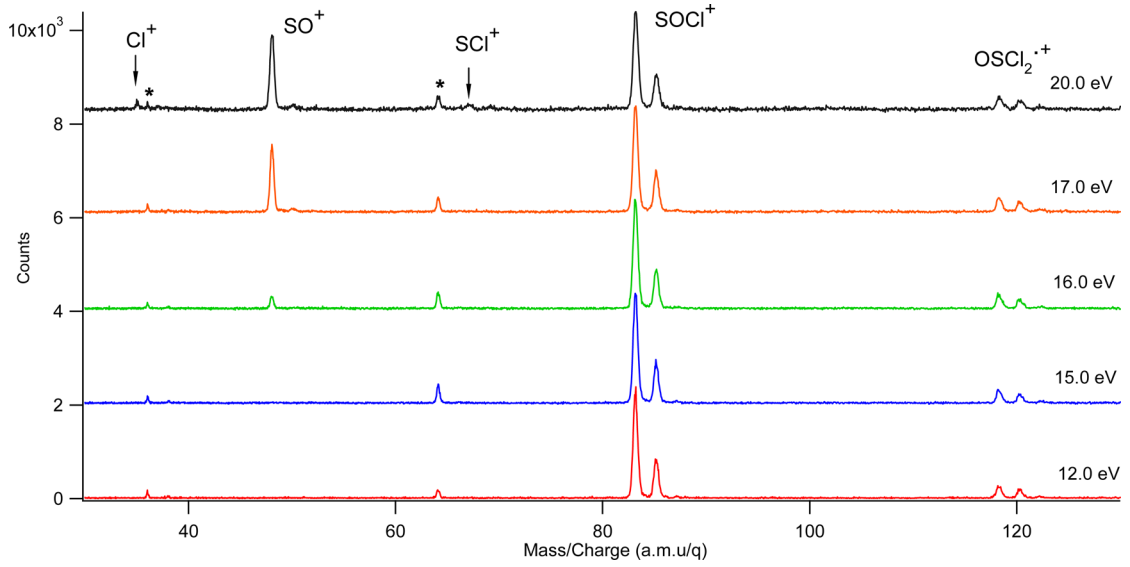

Figure 4. PEPICO spectra of $OSCl_2$ at at selected irradiation energies in the valence region. Bands marked with asterisks (*) may have originated from traces of $HCl^{\bullet+}$ and $SO_2^{\bullet+}$.

DOI: 10.1021/acs.jpca.5b02162
J. Phys. Chem. A 2015, 119, 8000−8009

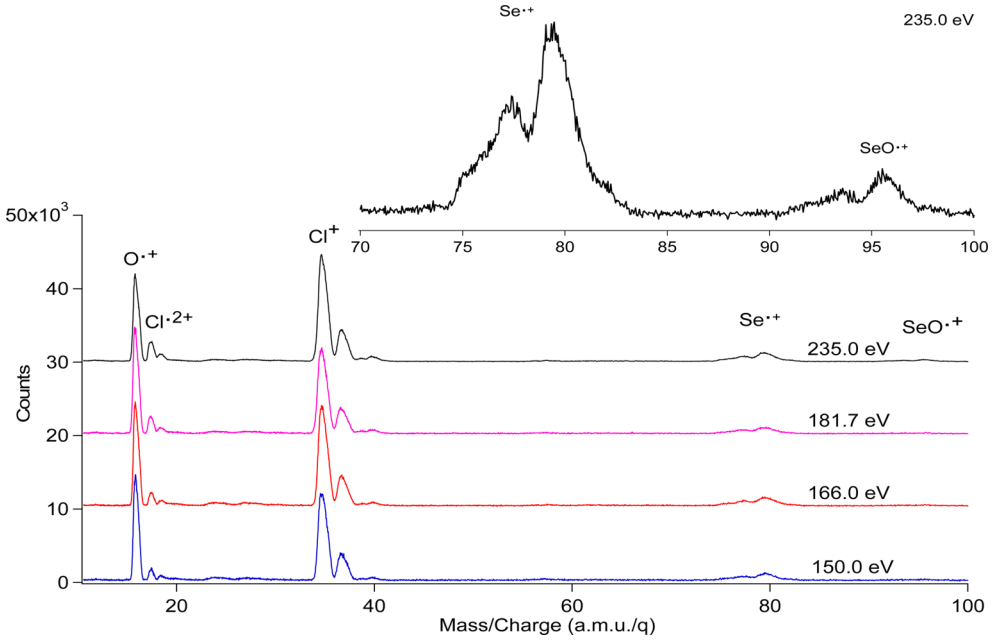

Figure 5. PEPICO spectra measured for $OSeCl_2$ at resonant Se 3p-, Cl 2p-, and Se 3s-edge absorptions.

excited species to unoccupied antibonding orbitals (Figure S5 in the Supporting Information).

3.3.2. PEPICO Spectra of $OSeCl_2$. The PEPICO spectra taken for $OSeCl_2$ at resonant Se 3p-, Cl 2p-, and Se 3s-edge absorptions are shown in Figure 5, together with a fragment assignment of the bands. In Table 3 the corresponding branching ratios are collected for the main fragment ions.

Table 3. Branching Ratios (%) for Fragment Ions Extracted from PEPICO Spectra Taken at Photon Energies around the Se 3p, Cl 2p and Se 3s Energies for $OSeCl_2$[a]

		branching ratios for selected ions				
electronic level	photon energy (eV)	$O^{\bullet+}$	$Cl^{\bullet2+}$	Cl^+	$Se^{\bullet+}$	$SeO^{\bullet+}$
Se 3p	164.0	34.1	5.3	47.2	13.5	
	166.0	32.4	5.1	48.6	13.8	
	172.0	30.4	5.3	49.9	14.4	
Cl 2p	181.7	37.3	6.5	45.8	10.4	
	202.7	36.9	7.3	45.8	10.0	
Se 3s	216.0	29.8	5.6	53.5	8.7	2.4
	235.0	29.8	6.9	52.2	8.8	2.2

[a]Ions with branching ratios lower than 1.0% are not listed. Contribution of the natural isotopomers of Cl and Se natural are summed together. The estimated experimental error was 10%.[52,53]

At these high photon energies, the main features in the PEPICO spectra are dominated by atomic ions such as O^+, Cl^+, and Se^+, while the only nonatomic charged fragment present in the PEPICO spectra belongs to the $SeO^{\bullet+}$ ion. The molecular ion, $OSeCl_2^{\bullet+}$, cannot be observed in any PEPICO spectra measured in these photon energies. Finally, a signal denoting the formation of the doubly charged atomic fragment, corresponding to both $Cl^{\bullet2+}$ isomers, is clearly observed.

The analysis of the PEPICO spectra of $OSeCl_2$ following Se 3p, Cl 2p, and Se 3s inner shell excitations reveals a preferential production of Cl^+ ions in all cases, with relative intensities varying between 45.0 and 53.0% approximately. The next most abundant ion is $O^{\bullet+}$ which reaches a branching value of 37%. The $Se^{\bullet+}$ ions, whose yields vary between 8% and 13% approximately, can also be observed. The intensity of the $Cl^{\bullet2+}$ doubly charged atomic fragment shows relative abundances on the order of about 5 at 7%. The heaviest fragment detected in the PEPICO spectra, $SeO^{\bullet+}$, also appears at some energies, having weak relative intensity (2% approximately) (Table 3). With respect to the last ion, it should be noted that only a singly charged molecular ion can produce the signal of the $SeO^{\bullet+}$ fragment.

A small increment in the Cl^+ peak intensity is observed by going toward higher energies. In addition, the smooth diminution in the intensities of the $O^{\bullet+}$ and $Se^{\bullet+}$ ion signals at increasing incident photon energies can also be noticed.

3.3.3. Total Ion Yield Spectra (TIY) of $OSCl_2$. The TIY spectrum of $OSCl_2$, measured near the S 2p-edge is shown in Figure S6 in the Supporting Information. Below the S 2p threshold (located at approximately 182.0 eV) the spectrum is dominated by a group of well-defined signals located at 166.5, 167.7, 169.0, 170.5, 171.9, and 173.2 eV. Two of these resonant transitions may correspond to transitions involving the spin−orbit split of the 2p term in the $2p_{1/2}$ and $2p_{3/2}$ levels in the excited species to unoccupied antibonding orbitals (mainly the σ^*_{S-Cl} (a′) and $\sigma^*_{S=O}$ orbitals, see Figure S7 in the Supporting Information). In the case of the simplest sulfide, H_2S, this splitting was reported to be 1.201 eV.[55]

The TIY spectrum recorded in the photon energy range between 198.0 and 240.0 eV is shown at the top of Supporting Information Figure S6. A simple feature without any fine structure can be seen in the Cl 2p region of $OSCl_2$, and the ionization edge can be observed at approximately 215.0 eV. In addition, a signal centered at 232.2 eV in Supporting Information Figure S6 can be assigned to the S 2s-edge.

3.3.4. PEPICO Spectra of $OSCl_2$. Several PEPICO spectra recorded near the S 2p-, Cl 2p-, and S 2s-edges are shown in Figure 6. The branching ratios for ion production obtained from the PEPICO spectra are given in Table 4. In all PEPICO spectra recorded in this work, the most intense peak is observed for the Cl^+ ion with relative intensities between 25.4% and 30.7%. The next most abundant ion is O^+ reaching branching

DOI: 10.1021/acs.jpca.5b02162
J. Phys. Chem. A 2015, 119, 8000−8009

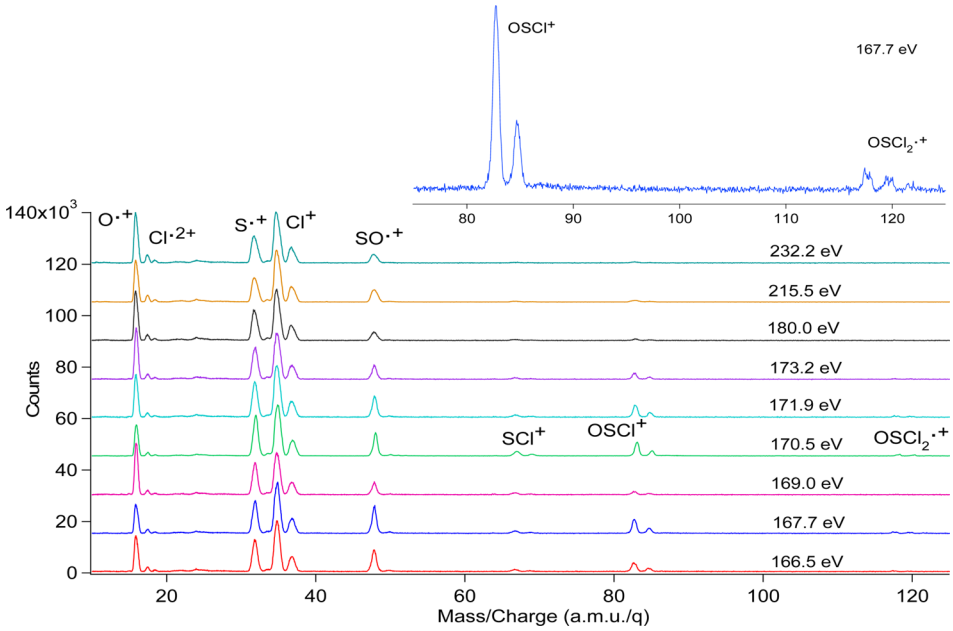

Figure 6. PEPICO spectra measured for $OSCl_2$ at resonant S 2p-, Cl 2p-, and S 2s-edge absorptions.

Table 4. Branching Ratios (%) for Fragment Ions Extracted from PEPICO Spectra Taken at Photon Energies around the S 2p, Cl 2p, and S 2s Energies for $OSCl_2$

		branching ratios at various m/z values (amu/q)[a,b]							
electronic edge	photon energy (eV)	$O^{\bullet+}$	$^{35}Cl^{\bullet2+}$[a]	$S^{\bullet+}$	$^{35}Cl^{+}$	$SO^{\bullet+}$	$S^{35}Cl^{+}$	$SO^{35}Cl^{+}$	$SO^{35}Cl_2^{\bullet+}$
S 2p	166.5	18.8	2.8	16.9	26.9	9.4	2.2	3.8	0.9
	167.7	16.1	2.4	17.4	27.8	10.8	2.1	4.8	0.9
	169.0	26.8	2.8	18.1	25.4	6.1	2.1	2.0	0.7
	170.5	15.5	2.2	19.8	27.5	8.7	2.9	4.3	0.9
	171.9	19.7	2.5	17.6	26.7	8.5	2.1	4.1	1.0
Cl 2p	173.2	26.1	2.8	18.0	27.4	6.4	1.5	2.4	
	180.0	26.3	3.1	18.0	29.0	5.1	1.4	1.2	
S 2s	215.5	23.4	3.5	16.0	30.7	7.5	1.2	1.4	
	232.2	25.4	4.1	16.7	28.1	5.6	1.5	1.4	

[a]Peaks for the corresponding naturally occurring isotopomer were observed. [b]The estimated experimental error was 10%.[52,53]

values between 15.5% and 26.8%. Another intense peak observed in the PEPICO spectra corresponds to the S^+ ion, with relative abundances between 16.0% and 19.8%. A signal for the $SO^{\bullet+}$ ion also appears in these spectra, showing relative intensities between 5.1% and 10.8%. Other less abundant fragments are $OSCl^+$ (<4.8%), SCl^+ (<2.9%), and $Cl^{\bullet2+}$ (<4.1%).

The parent ion, $OSCl_2^{\bullet+}$, can be observed as a very low-intenseity signal in some PEPICO spectra and shows the characteristic chlorine isotopic distribution. In the reported electron-impact mass spectrum of $OSCl_2$ measured at an ionization energy of 70 eV, the same ions could be observed that are in the photon impact mass spectra, with the exception of the $O^{\bullet+}$ ion.[56] The $OSCl^+$ is the most important ion observed in the electron impact mass spectra, followed in abundance by Cl^+, $SO^{\bullet+}$, $S^{\bullet+}$, $OSCl_2^{\bullet+}$, and finally SCl^+.

The intensity signals of the heavier ions SCl^+, $OSCl^+$, and $OSCl_2^{\bullet+}$ are slightly depressed by going toward higher energies. The variation in the peak intensity corresponding to the $SO^{\bullet+}$ ion seems to be correlated with the opposite tendency observed in the signal intensity of the $O^{\bullet+}$. In addition, the peak corresponding to the $SO^{\bullet+}$ fragment becomes broad and less resolved by going from S 2p to the S 2s region denoting the importance of Auger-induced double-ionization and fragmentation processes that lead to the formation of fragment ions with higher kinetic energy.

3.3.5. PEPIPICO Spectra of $OSeCl_2$ and $OSCl_2$. In the PEPIPICO spectra, one electron and two positive ions were recorded in a correlated way at several photon energies near the Se 3p-, S 2p-, and Cl 2p-edges of the $OSeCl_2$ and $OSCl_2$ molecules. This type of spectra reflects mainly pairs of singly charged fragment ions that originated from the fragmentation of the doubly charged parent molecule.

In the case of $OSeCl_2$, the most intense islands observed in the PEPIPICO spectra correspond to double coincidences involving the m/z values of 16, 35, and 80 amu/q. These coincidences can be observed in the PEPIPICO spectra with a nondefined shape indicating the contribution of several dissociation processes. Thus, the coincidence of the $O^{\bullet+}$ ions with the Cl^+ ions and the coincidence between $O^{\bullet+}$ and $Se^{\bullet+}$ ions and between Cl^+ and $Se^{\bullet+}$ ions were observed. Fragmentation processes leading to the formation of Cl^+ and $SeO^{\bullet+}$ ions are also observed in the PEPIPICO spectra. The importance of the contribution of double coincidences involving the Cl^+ ion can be inferred from the projection spectrum over the Cl^+ arriving time (Figure 7). The contour

DOI: 10.1021/acs.jpca.5b02162
J. Phys. Chem. A 2015, 119, 8000−8009

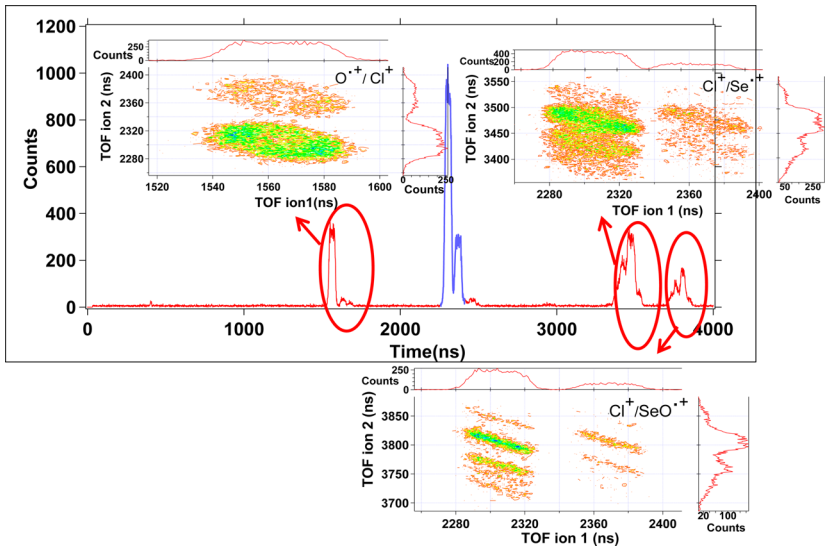

Figure 7. Projection spectrum over the Cl^+ arriving time recorded at 216.0 eV for $OSeCl_2$. Contour plots for the double-coincidence islands between $O^{\bullet+}/Cl^+$ (top left), $Cl^+/Se^{\bullet+}$ (top right), and $Cl^+/SeO^{\bullet+}$ (bottom) ions derived from the PEPIPICO spectrum of $OSeCl_2$ are also shown.

plot of the most intense double coincidences, $O^{\bullet+}/Cl^+$, $Cl^+/Se^{\bullet+}$, and $Cl^+/SeO^{\bullet+}$, are shown in Figure 7. In addition, the $^{35}Cl^+/^{37}Cl^+$ coincidence was observed in the PEPIPICO spectra as a low-intensity signal. On the other hand, fragmentation processes in $OSCl_2$ leading to the formation of double coincidences involving the m/z values of 16, 32, and 35 amu/q appear as the most intense in the PEPIPICO spectra like in the selenium analogue $OSeCl_2$ where in this case the PEPIPICO spectra are dominated by the ions with m/z values of 16, 35, and 80 amu/q.

The coincidences $O^{\bullet+}/Cl^+$ and $O^{\bullet+}/S^{\bullet+}$ represent the most intense islands in the 220.0 eV PEPIPICO (see Figure 8)

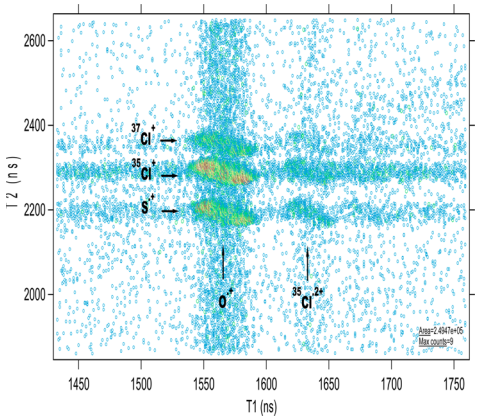

Figure 8. Enlargement of the PEPIPICO spectrum of $OSCl_2$ obtained at 220.0 eV photon energy in the ranges m/z 16−18.5 and 32−37 amu/q in the T1 and T2 domains, respectively.

spectrum and in the other PEPIPICO measured. The coincidence between $S^{\bullet+}$ and Cl^+ ions is also observed as an intense island. Fragmentation processes leading to the formation of Cl^+ and $SO^{\bullet+}$ ions and $^{35}Cl^+$ with $^{37}Cl^+$ ions are also observed as low-intensity islands in all energy ranges (Figure 9). Very low-intensity $Cl^{\bullet2+}/S^+$ and $Cl^{\bullet2+}/Cl^+$ islands are observed and should have originated in fragmentation processes arising from at least triply charged $OSCl_2$.

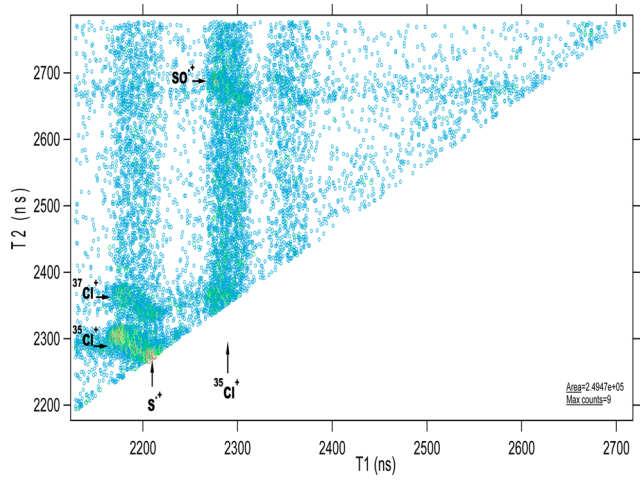

Figure 9. Enlargement of the PEPIPICO spectrum of $OSCl_2$ obtained at 220.0 eV photon energy in the ranges m/z 32−37 and 35−48 amu/q in the T1 and T2 domains, respectively.

4. CONCLUSIONS

Photoelectron spectroscopy and photoionization studies using synchrotron radiation on selenium oxychloride demonstrate that the incidence of photons with energy in the valence region causes the ionization of the molecule, and together with the molecular ion, a series of fragmentation channels are opened, mainly leading to the formation of $OSeCl^+$, $SeCl_2^{\bullet+}$, and $SeCl^+$ ions. When the energy of photons is increased, the ionization channel for the formation of $SeO^{\bullet+}$ is opened. In the PEPICO spectra of its analogue $OSCl_2$, the $OSCl^+$ signal dominates the spectra, like in $OSeCl_2$ where in this case the photofragmentation is dominated by the $OSeCl^+$ ion. In addition, the ionization channel for the formation of SO^+ is opened to an energy value similar to that of the selenium analogue, and a marked enhancement in the intensity of this signal could be observed when the sample is irradiated with photons of higher energy like in $OSeCl_2$.

The inner shell Se 3p, Cl 2p, and Se 3s electronic regions of selenium oxychloride together with S 2p, Cl 2p, and S 2s electronic regions of thionyl chloride have been studied by

DOI: 10.1021/acs.jpca.5b02162
J. Phys. Chem. A 2015, 119, 8000−8009

using tunable synchrotron radiation. Total ion yield (TIY) and photoelectron−photoion coincidence (PEPICO) spectra were measured. Some differences in the photofragmentation behavior in the shallow-core regions between the sulfur- and selenium-containing compound were observed. The $OSeCl_2^{\bullet+}$ ion cannot be observed in any PEPICO spectra measured in these photon energies with $SeO^{\bullet+}$ being the heaviest fragment detected. On the other hand, the $OSCl_2^{\bullet+}$ ion can be observed as a very low-intensity signal in some PEPICO spectra measured around the S 2p-edge. In addition, other molecular fragments observed with high relative intensities in all the photon impact mass spectra measured are $SO^{\bullet+}$, SCl^+, and $OSCl^+$. The relative abundances of the photodissociation products Cl^+, $O^{\bullet+}$, and $Se^{\bullet+}$ in $OSeCl_2$ appear as the most intense in the PEPICO spectra like in that of the sulfur analogue $OSCl_2$ where in this case the photofragmentation is dominated by the Cl^+, $O^{\bullet+}$, and $S^{\bullet+}$ ions. This behavior for the two related species is illustrated in Figure S8 (see Supporting Information), where the similitude of the PEPICO spectra at similar energies is apparent. The analysis of PEPIPICO spectra for both molecules studied reveals double coincidence signals involving atomic ions.

■ ASSOCIATED CONTENT

Supporting Information

Main characters of the 11 highest occupied molecular orbitals of $OSeCl_2$ in Figure S1. Figure S2 giving the He I photoionization mass spectrum (PIMS) of $OSeCl_2$. The TIY spectrum of $OSeCl_2$ in the photon energy range 150.0−250.0 eV in Figure S3. The schematic representations of the three lower energy unoccupied molecular orbitals for $OSeCl_2$ and $OSCl_2$ in Figures S4 and S7, respectively. Figure S5 giving the TIY spectrum of $OSeCl_2$ in the photon energy range 51.0−56.5 eV and Figure S6 giving the TIY spectra of $OSCl_2$ in the S 2p, Cl 2p, and S 2s regions. Figure S8 giving the PEPICO spectra measured for $OSeCl_2$ and $OSCl_2$ at 216.0 and 215.5 eV, respectively. The Supporting Information is available free of charge on the ACS Publications website at DOI: 10.1021/acs.jpca.5b02162.

■ AUTHOR INFORMATION

Corresponding Author

*E-mail: carlosdv@quimica.unlp.edu.ar.

Notes

The authors declare no competing financial interest.

■ ACKNOWLEDGMENTS

M.G., M.F.E., R.M.R., and C.O.D.V. are members of the Carrera del Investigador of CONICET, and L.S.R.P. is a postdoctoral fellow of CONICET. This work has been largely supported by the Brazilian Synchrotron Light Source (LNLS). The authors wish to thank Arnaldo Naves de Brito and his research group for fruitful discussions and generous collaboration during their several stays in Campinas and the TGM beamline staff for their assistance throughout the experiments. They also are in debt to the Agencia Nacional de Promoción Científica y Tecnológica (ANPCyT), Consejo Nacional de Investigaciones Científicas y Técnicas (CONICET), and the Comisión de Investigaciones Científicas de la Provincia de Buenos Aires (CIC), República Argentina, for financial support. They also thank the Facultad de Ciencias Exactas, Universidad Nacional de La Plata, República Argentina, for financial support. The authors wish to acknowledge the support of the Chinese Academy of Sciences for work in the Institute of Chemistry of the Chinese Academy of Science in Beijing.

■ REFERENCES

(1) Reilly, C. *Selenium in Food and Health*, 2nd ed.; Springer: New York, 2006.

(2) Hayakawa, T.; Nagaya, K.; Yamamoto, I.; Ohmasa, Y.; Yao, M.; Nomura, M. Photoelectron Photoion Coincidence Measurements of Selenium Cluster Beam. I. Evidence for the Coulomb Explosion. *J. Phys. Soc. Jpn.* **2000**, *69*, 2039−2048.

(3) Hayakawa, T.; Nagaya, K.; Hamada, K.; Ohmasa, Y.; Yao, M. Photoelectron Photoion Coincidence Measurements of Selenium Cluster Beam. II. Photon Energy Dependence. *J. Phys. Soc. Jpn.* **2000**, *69*, 2850−2858.

(4) Yao, M.; Hayakawa, T.; Nagaya, K.; Hamada, K.; Ohmasa, Y.; Nomura, M. A New Method for the Size-Selective EXAFS of Neutral Free Clusters. *J. Synchrotron Radiat.* **2001**, *8*, 542−544.

(5) Nagaya, K.; Yao, M.; Hayakawa, T.; Ohmasa, Y.; Kajihara, Y.; Ishii, M.; Katayama, Y. Size-Selective Extended X-ray Absorption Fine Structure Spectroscopy of Free Selenium Clusters. *Phys. Rev. Lett.* **2002**, *89*, 243401−243404.

(6) Chau, F. T.; Lee, E. P. F.; Wang, D. C. Theoretical Study of the Vibrational Structure of the He I Photoelectron Spectrum of H_2Se. *J. Phys. Chem. A* **1997**, *101*, 1603−1608.

(7) Frost, D. C.; Lee, S. T.; McDowell, C. A. Photoelectron Spectra of OCSe, SCSe, and CSe_2. *J. Chem. Phys.* **1973**, *59*, 5484−5493.

(8) Cradock, S.; Duncan, W. Photoelectron Spectra of OCSe and SCSe. *J. Chem. Soc., Faraday Trans. 2* **1975**, *71*, 1262−1268.

(9) Cradock, S.; Donovan, R. J.; Duncan, W.; Gillespie, H. M. Vacuum Ultraviolet Spectrum of Carbonyl Selenide, OCSe. *Chem. Phys. Lett.* **1975**, *31*, 344−347.

(10) Meija, J.; Beck, T. L.; Caruso, J. A. Interpretation of Alkyl Diselenide and Delenosulfenate Mass Spectra. *J. Am. Soc. Mass Spectrom.* **2004**, *15*, 1325−1332.

(11) Borkar, S.; Sztáray, B.; Bodi, A. Energetics and Dissociation Pathways of Dimethyl Disulfide and Dimethyl Diselenide using Photoelectron Photoion Coincidence Spectroscopy. *J. Electron Spectrosc. Relat. Phenom.* **2014**, *196*, 165−172.

(12) Erk, B.; Rolles, D.; Foucar, L.; Rudek, B.; Epp, S. W.; Cryle, M.; Bostedt, C.; Schorb, S.; Bozek, J.; Rouzee, A.; et al. Inner-Shell Multiple Ionization of Polyatomic Molecules with an Intense X-Ray Free-Electron Laser Studied by Coincident Ion Momentum Imaging. *J. Phys. B: At., Mol. Opt. Phys.* **2013**, *46*, 164031−164043.

(13) Erk, B.; Rolles, D.; Foucar, L.; Rudek, B.; Epp, S. W.; Cryle, M.; Bostedt, C.; Schorb, S.; Bozek, J.; Rouzee, A.; et al. Ultrafast Charge Rearrangement and Nuclear Dynamics upon Inner-Shell Multiple Ionization of Small Polyatomic Molecules. *Phys. Rev. Lett.* **2013**, *110*, 53003−53007.

(14) Geronés, M.; Erben, M. F.; Romano, R. M.; Cavasso Filho, R. L.; Della Védova, C. O. Dissociative Photoionization of Methyl Thiochloroformate, $ClC(O)SCH_3$, Following Sulfur 2p, Chlorine 2p, Carbon 1s, and Oxygen 1s Excitations. *J. Phys. Chem. A* **2012**, *116*, 7498−7507.

(15) Rodríguez Pirani, L. S.; Erben, M. F.; Geronés, M.; Romano, R. M.; Cavasso Filho, R. L.; Ma, C.; Ge, M.; Della Védova, C. O. Electronic Properties of $FC(O)SCH_2CH_3$. A Combined Helium(I) Photoelectron Spectroscopy and Synchrotron Radiation Study. *J. Phys. Chem. A* **2014**, *118*, 5950−5960.

(16) Gregory, D.; Hargittai, I.; Kolonits, M. The Molecular Structure of Selenium Oxychloride as Studied by Electron Diffraction. *J. Mol. Struct.* **1976**, *31*, 261−267.

(17) Zharskii, I. M.; Zasorin, E. Z.; Spiridonov, V. P.; Novikov, G. I. Electron Diffraction Study of Structure of $SeOCl_2$ Molecule. *Vestn. Mosk. Univ. Khim.* **1977**, *18*, 166−169.

(18) Westphal, G. H.; Rosenberger, F. Infrared Spectrum of Matrix-Isolated $SeOCl_2$. *J. Mol. Spectrosc.* **1980**, *83*, 355−359.

DOI: 10.1021/acs.jpca.5b02162
J. Phys. Chem. A 2015, 119, 8000−8009

(19) Sheldon, J. C.; Tyree, S. Y. The Donor Properties of $POCl_3$, $SeOCl_2$, CH_3COCl, $SOCl_2$ and $VOCl_3$. *J. Am. Chem. Soc.* **1959**, *81*, 2290−2296.
(20) Smith, G. B. L. Selenium Oxychloride as a Solvent. *Chem. Rev.* **1938**, *23*, 165−185.
(21) Silva, A. R.; Martins, M.; Freitas, M. M. A.; Valente, A.; Freire, C.; de Castro, B.; Figueiredo, J. L. Immobilisation of Amine-Functionalised Nickel(II) Schiff Base Complexes onto Activated Carbon Treated with Thionyl Chloride. *Microporous Mesoporous Mater.* **2002**, *55* (3), 275−284.
(22) Kirk, R. E.; Othmer, D. F. *Encyclopedia of Chemical Technology*, 3rd ed.; Wiley: New York, 1983; Vol. *22*.
(23) Li, M. Thionyl Chloride - A Versatile Reagent. *Synlett* **2007**, *16*, 2605−2606.
(24) Hitchcock, A. P.; Bodeur, S.; Tronc, M. Sulfur and Chlorine K-shell X-Ray Absorption Spectra of SCl_2, S_2Cl_2, $SOCl_2$, and SO_2Cl_2. *Chem. Phys.* **1987**, *115*, 93−101.
(25) Bowen, K. P.; Stolte, W. C.; Lago, A. F.; Dávalos, J. Z.; Piancastelli, M. N.; et al. Partial-Ion-Yield Studies of $SOCl_2$ Following X-Ray Absorption around the S and Cl K Edges. *J. Chem. Phys.* **2012**, *137*, 204313.
(26) Lira, A. C.; Rodrigues, A. R. D.; Rosa, A.; Gonçalves da Silva, C. E. T.; Pardine, C.; Scorzato, C.; Wisnivesky, D.; Rafael, F.; Franco, G. S.; Tosin, G. et al. First Year Operation of the Brazilian Sinchrotron Light Source. In *EPAC98, European Particle Accelerator Conference, Stockholm*; Institute of Physics: London, 1998.
(27) Craievich, A. F.; Rodrigues, A. R. The Brazilian Synchrotron Light Source. *Hyperfine Interact.* **1998**, *113*, 465−475.
(28) Rodrigues, A. R. D.; Craievich, A. F.; Gonçalves da Silva, C. E. T. *J.* Commissioning and Operation of the First Brazilian Synchrotron Light Source. *J. Synchrotron Radiat.* **1998**, *5*, 1157−1161.
(29) Cavasso Filho, R. L.; Homen, M. G. P.; Fonseca, P. T.; Naves de Brito, A. A Synchrotron Beamline for Delivering High Purity Vacuum Ultraviolet Photons. *Rev. Sci. Instrum.* **2007**, *78*, 115104−115108.
(30) Cavasso Filho, R. L.; Lago, A. F.; Homem, M. G. P.; Pilling, S.; Naves de Brito, A. Delivering High-Purity Vacuum Ultraviolet Photons at the Brazilian Toroidal Grating Monochromator (TGM) Beamline. *J. Electron Spectrosc. Relat. Phenom.* **2007**, *156−158*, 168−171.
(31) Frasinski, L. J.; Stankiewicz, M.; Randall, K. J.; Hatherly, P. A.; Codling, K. Dissociative Photoionization of Molecules Probed by Triple Coincidence; Double Time-of-Flight Techniques. *J. Phys. B: At. Mol. Phys.* **1986**, *19*, L819−L824.
(32) Eland, J. H. D. The Dynamics of Three-Body Dissociations of Dications Studied by the Triple Coincidence Technique PEPIPICO. *Mol. Phys.* **1987**, *61*, 725−745.
(33) Burmeister, F.; Coutinho, L. H.; Marinho, R. R. T.; Homem, M. G. P.; de Morais, M. A. A.; Mocellin, A.; Björneholm, O.; Sorensen, S. L.; Fonseca, P. T.; Lindgren, A.; et al. Description and Performance of an Electron-Ion Coincidence TOF Spectrometer used at the Brazilian Synchrotron Facility LNLS. *J. Electron Spectrosc. Relat. Phenom.* **2010**, *180*, 6−13.
(34) Zeng, X.; Ge, M.; Sun, Z.; Bian, J.; Wang, D. Gaseous Nitryl Azide N_4O_2: A Joint Theoretical and Experimental Study. *J. Mol. Struct.* **2007**, *840*, 59−65.
(35) Zeng, X.; Yao, L.; Wang, W.; Liu, F.; Sun, Q.; Ge, M.; Sun, Z.; Zhang, J.; Wang, D. Electronic Structures of Acyl Nitrites and Nitrates. *Spectrochim. Acta, Part A* **2006**, *64*, 949−955.
(36) Yao, L.; Zeng, X. Q.; Ge, M.; Wang, W. G.; Sun, Z.; Du, L.; Wang, D. X. First Experimental Observation of Gas-Phase Nitrosyl Thiocyanate. *Eur. J. Inorg. Chem.* **2006**, *2006*, 2469−2475.
(37) Xiaoqing, Z.; Fengyi, L.; Qiao, S.; Maofa, G.; Jianping, Z.; Xicheng, A.; Lingpeng, M.; Shijun, Z.; Dianxun, W. Reaction of AgN_3 with $SOCl_2$: Evidence for the Formation of Thionyl Azide, $SO(N_3)_2$. *Inorg. Chem.* **2004**, *43*, 4799−4801.
(38) Wang, W.; Yao, L.; Zeng, X.; Ge, M.; Sun, Z.; Wang, D.; Ding, Y. Evidence of the Formation and Conversion of Unstable Thionyl Isocyanate: Gas-Phase Spectroscopic Studies. *J. Chem. Phys.* **2006**, *125*, 234303.
(39) Li, Y.; Zeng, X.; Sun, Q.; Li, H.; Ge, M.; Wang, D. Electronic Structure of H_2CS_3 and H_2CS_4: An Experimental and Theoretical Study. *Spectrochim. Acta, Part A* **2007**, *66*, 1261−1266.
(40) Wang, W.; Ge, M.; Yao, L.; Zeng, X.; Sun, Z.; Wang, D. Gas-Phase Spectroscopy of the Unstable Sulfur Diisocyanate Molecule $S(NCO)_2$. *ChemPhysChem* **2006**, *7*, 1382−1387.
(41) Zeng, X.; Wang, D. Novel Gaseous Transient Species: Generation and Characterization. *Sci. China, Ser. B: Chem.* **2007**, *50*, 145−169.
(42) Nakatsuji, H.; Hirao, K. Cluster Expansion of the Wavefunction Symmetry-Adapted-Cluster Expansion, its Variational Determination and Extension of Open-Shell Orbital Theory. *J. Chem. Phys.* **1978**, *68* (5), 2053−2065.
(43) Nakatsuji, H. Cluster Expansion of the Wavefunction. Excited States. *Chem. Phys. Lett.* **1978**, *59* (2), 362−364.
(44) Cederbaum, L. S.; Domcke, W. Theoretical Aspects of Ionization Potentials and Photoelectron Spectroscopy: A Green's Function Approach. *Adv. Chem. Phys.* **1977**, *36*, 205−344.
(45) Frisch, M. J.; Trucks, G. W.; Schlegel, H. B.; Scuseria, G. E.; Robb, M. A.; Cheeseman, J. R.; Montgomery, J. A., Jr.; Vreven, T.; Kudin, K. N.; Burant, J. C.; et al. *Gaussian, Revision B.04*; Gaussian, Inc.: Pittsburgh, PA, 2003.
(46) Chadwick, D.; Frost, D. C.; Herring, F. G.; Katrib, A.; Mcdowell, C. A.; Mclean, R. A. N. Photoelectron Spectra of Sulfuryl and Thionyl Halides. *Can. J. Chem.* **1973**, *51*, 1893−1905.
(47) Deleuze, M. S. Valence One-Electron and Shake-Up Ionization Bands of Polycyclic Aromatic Hydrocarbons. II. Azulene, Phenanthrene, Pyrene, Chrysene, Triphenylene, and Perylene. *J. Chem. Phys.* **2002**, *116*, 7012−7026.
(48) Deleuze, M. S. Valence One-Electron and Shake-Up Ionization Bands of Polycyclic Aromatic Hydrocarbons. III. Coronene, 1.2,6.7-Dibenzopyrene, 1.12-Benzoperylene, Anthanthrene. *J. Phys. Chem. A* **2004**, *108*, 9244−9259.
(49) Deleuze, M. S. Valence One-Electron and Shake-Up Ionisation Bands of Polycyclic Aromatic Hydrocarbons. IV. The Dibenzanthracene Species. *Chem. Phys.* **2006**, *329*, 22−38.
(50) Mayer, P. M.; Baer, T. The Heat of Formation of $CISO^+$. *Chem. Phys. Lett.* **1996**, *261*, 155−159.
(51) Borkar, S.; Ooka, L.; Bodi, A.; Gerber, T.; Sztáray, B. Dissociative Photoionization of Sulfur Chlorides and Oxochlorides: Thermochemistry and Bond Energies Based on Accurate Appearance Energies. *J. Phys. Chem. A* **2010**, *114*, 9115−9123.
(52) Boechat-Roberty, H. M.; Pilling, S.; Santos, A. C. F. Destruction of Formic Acid by Soft X-Rays in Star-Forming Regions. *Astron. Astrophys.* **2005**, *438*, 915−922.
(53) Pilling, S.; Andrade, D. P. P. Employing Soft X-Rays in Experimental Astrochemistry. *X-Ray Spectroscopy*, Sharma, S. K., Ed.; InTech: Rijeka, Croatia, 2012. Available from http://www.intechopen.com/books/x-ray-spectroscopy/employing-soft-x-rays-in-experimental-astrochemistry.
(54) Nenner, I.; Beswick, J. A. Molecular Photodissociation and Photoionization. In *Handbook on Synchrotron Radiation*; Marr, G. V., Ed.; Elsevier Science/North-Holland: Amsterdam, 1987; Vol. *2*, pp 355−462.
(55) Svensson, S.; Naves de Brito, A.; Keane, M. P.; Correia, N.; Karlsson, L. Observation of an Energy Shift in the $S2p_{3/2}$−$S2p_{1/2}$ Spin-Orbit Splitting between X-Ray Photoelectron and Auger-Electron Spectra for the H_2S Molecule. *Phys. Rev. A: At., Mol., Opt. Phys.* **1991**, *43*, 6441−6443.
(56) Stein, S. E. Mass Spectra. *NIST Standard Reference Database Number 69*; NIST Mass Spec. Data Center, National Institute of Standards and Technology: Gaithersburg, MD, 2003 (http://webbook.nist.gov).

DOI: 10.1021/acs.jpca.5b02162
J. Phys. Chem. A 2015, 119, 8000−8009